



Effect of deacetylation on wicking behavior of co-electrospun cellulose acetate/polyvinyl alcohol nanofibers blend

Zeeshan Khatri, Kai Wei, Byoung-Suhk Kim, Ick-Soo Kim*

Nano Fusion Technology Research Group, Faculty of Textile Science and Technology, Shinshu University, Ueda, Nagano 386-8567, Japan

ARTICLE INFO

Article history:

Received 22 August 2011

Received in revised form 7 October 2011

Accepted 17 October 2011

Available online 25 October 2011

Keywords:

Cellulose acetate nanofibers

Polyvinyl alcohol nanofibers

Deacetylation

Rate of wicking

Co-electrospinning

ABSTRACT

Cellulose acetate (CA) nanofibers webs deserve a special attention because of their very good water retention properties. CA nanofibers based biosensor in certain application come into contact with various liquids and requires high degree of wicking rate to transport liquid to its destination. Cellulose acetate (CA)/polyvinyl alcohol (PVA) blended nanofibers were prepared via co-electrospinning using double nozzle for jetting cellulose acetate and polyvinyl alcohol independently. The CA/PVA blend nanofibers webs were deacetylated in aqueous alkaline solution to convert CA in to regenerated cellulose and to remove PVA nanofibers from the raw web. The resultant nanofibers webs were characterized by wicking rate, water contact angle, SEM and FTIR analysis. The results revealed that by varying concentration of PVA solution enhances the wicking rate. Such a nanofibers web may be used in biosensor strip and other medical applications where the high wicking rates are desired.

© 2011 Elsevier Ltd. All rights reserved.

1. Introduction

Producing nanofibers via electrospinning is not new. However, blending different polymers and attempts are being undertaken towards the development of multi characteristic nanofibers to fulfill stringent requirements. Cellulose acetate (CA) nanofibers webs deserve a special attention because of their very good water retention properties. The water retention per fibrous mass for the electrospun CA nanofibers web is nearly ten times higher than that for fabrics (Liu & Hsieh, 2002). CA – a widely studied and characterized in terms of affinity membrane and filtration (Ma, Kotaki, & Ramakrishna, 2005; Ma & Ramakrishna, 2008), capillary absorption models (Callegari, Tyomkin, Kornev, Neimark, & Hsieh, 2011), deacetylation of nanofibers (Son, Youk, Lee, & Park, 2004). Electrospun fibrous webs have wide applications as bio-materials for tissue engineering and scaffolds (Du & Hsieh, 2008; Du & Hsieh, 2009; Katti, Robinson, Ko, & Laurencin, 2004).

CA nanofibers based biosensor (Liu, Tan, Hu, Li, & Chen, 2010; Wang et al., 2004) in certain application come into contact with various liquids and require high degree of wicking rate to transport liquid to its destination (Callegari et al., 2011). As a matter of fact that the CA nanofibers have limited water wicking due to presence of acetyl groups, therefore CA nanofibers are

converted into regenerated cellulose (RC) to obtain satisfactory degree of wicking (Liu & Hsieh, 2002). The process of CA conversion into RC by deacetylation is very common that may be carried by treating CA nanofibers either in aqueous NaOH/EtOH solution for shorter period (Liu & Hsieh, 2002) or aqueous NaOH solution for longer time span (Callegari et al., 2011). The degree of substitution has been reported to complete by both methods. Yaser, Mohammed, Eisa, and Bothaina (2010), investigated the effect of thermal treatment of CA nanofibrous membranes at temperatures up to 208 °C in various conditions, followed by deacetylation for conversion of CA into RC nanofibers using 0.5 M NaOH aqueous solution. To enhance even high wicking rate of RC nanofibers, the CA nanofibers and blended with polyvinyl alcohol (PVA) nanofibers were co-electrospun simultaneously, followed by deacetylation to remove PVA nanofibers and convert CA into RC nanofibers. PVA is extremely hydrophilic and soluble in water (Tsukada, Freddi, & Crighiton, 1994). The PVA itself readily reacts with different cross-linking agents to form a gel (Hodge, Edward, & Simon, 1996). The water solubility is dependent on degrees of hydrolysis (DH). The effect of various DH on electrospinning has been discussed (Park et al., 2010). The fabrication and characterization of CA/PVA blends nanofibrous nonwoven mats have been studied by (Ding, Kimura, Sato, Fujita, & Shiratori, 2004) in terms of their morphologies and mechanical properties.

The aim of this research was to enhance the wicking rate and to investigate the effect of deacetylation on wicking behavior of CA/PVA nanofibers webs. PVA nanofibers were produced from two concentrations 10% and 15% (wt%), each was co-electrospun with 17% (wt%) CA nanofibers and collected on same collector/drum.

* Corresponding author at: Nano Fusion Technology Research Group, Faculty of Textile Science and Technology, Shinshu University, 3-15-1 Tokida, Ueda City, Nagano 386-8567, Japan. Tel.: +81 268 21 5439; fax: +81 268 21 5482.

E-mail address: kim@shinshu-u.ac.jp (I.-S. Kim).

The use of PVA nanofibers were interim since the CA/PVA blend nanofiber webs were deacetylated to remove PVA component and convert CA nanofibers into RC nanofibers. The resultant nanofibers webs were characterized by wicking rate, water contact angle, FTIR and SEM analysis and compared to untreated nanofibers webs.

2. Materials and methods

2.1. Materials

Cellulose acetate, CA (39.8% acetyl content having average Mw = 30 kDa) and polyvinyl alcohol, PVA (87–89% hydrolyzed, average Mw = 124–186 kDa) were obtained from Aldrich Chemical Company, and used without further purification.

2.2. Co-electrospinning

A high-voltage power supply (Har-100*12, Matsusada Co., Tokyo, Japan), capable of generating voltages up to 100 kV, was used as the source of the electric field. The concentration of CA was 17% by weight and prepared in acetone/dimethyl formamide (DMF) with 2:1 by weight, while the PVA solutions were prepared in distilled water with two concentrations 10% and 15% by weight. CA and PVA solutions were co-electrospun independently and simultaneously onto a rotating metallic drum/collector at room temperature. Each solution was supplied through a plastic syringe attached to a capillary tip with an inner diameter of 0.6 mm. The copper wire connected to a positive electrode (anode) was inserted into the polymer solution, and a negative electrode (cathode) was attached to a metallic collector. The voltage was fixed at 12.5 kV for CA and 12 kV for PVA. The distance between the capillary tip and the collector was fixed to be 15 cm for both CA and PVA, and the plastic syringes were placed at an angle of 10° from the horizontal direction. Three types of nanofiber webs were prepared: (1) CA nanofiber without PVA nanofibers, (2) CA nanofibers with 10% PVA nanofibers, and (3) CA nanofibers with 15% PVA nanofibers. Electrospinning was continued till the thickness of nanofiber web was achieved between 40 μm and 60 μm range. All nanofiber webs were air dried for at least 48 h and then subjected to deacetylation.

2.3. Deacetylation

In order to remove acetyl groups from the CA nanofibers and remove PVA content from the CA nanofibers webs, deacetylation was carried out by aqueous hydrolysis (Callegari et al., 2011) in 0.05 M NaOH solution for 30 h at room temperature and thoroughly rinsed off in distilled water until the pH of nanofiber webs reached to 7, followed by drying at 50 °C for 4 h. Additionally, pure PVA 10% nanofibers and pure PVA 15% nanofibers were dissolved separately to ensure their solubility in 0.05 M NaOH solution for deacetylation of CA/PVA nanofibers blend.

2.4. Measurements

2.4.1. Wicking rate

Wicking rate (the increase in height of wicking front per second) was assessed by hanging samples vertically over the petri dish containing dye solution. 1% (w/v) dye solution was prepared with CI Reactive Blue 19 (Sumfix Brilliant Blue R, Sumitomo Chemicals, Japan) dissolved in distilled water. The sample size of nanofibers web was cut into 20 mm height and 5 mm width and fixed in a upright stationary clamp, beneath, a petri dish containing dye solution was kept on the jack movable up and down. The lower end of sample was 5 mm below the liquid surface during the wicking test and remaining 15 mm was observed for wicking rise. The stop watch started as soon as the surface layer of dye solution touched

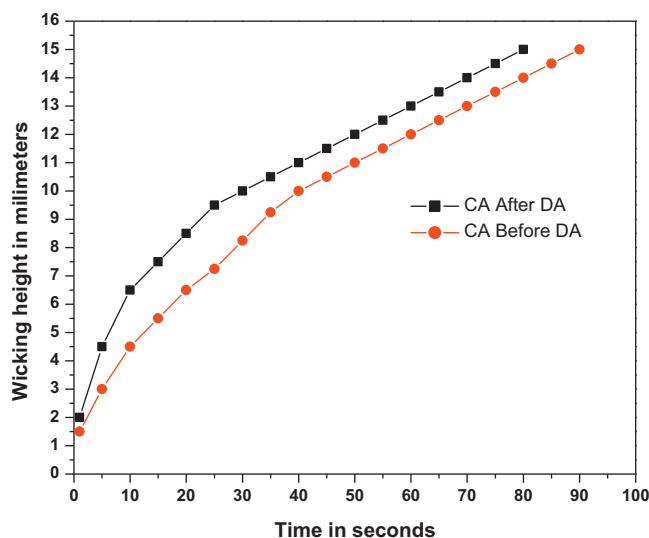


Fig. 1. Wicking rate for CA without PVA, before and after deacetylation.

the bottom edge of the vertically suspended sample. Simultaneously, a Camera (Canon with 8 megapixel) capable of capturing multiple shots at the rate of one shot per second, was also started. The wicking test was lasted for either maximum 90 s or the wicking front reaches the height of maximum 15 mm, whichever reached first. The reason for setting up two different sets of conditions was that some samples having very high wicking could reach 15 mm height in less than 90 s and some of the samples, due to lack of wicking property, could not reach the height of 15 mm in more than 90 s. The multishot images were further evaluated by using Adobe Photoshop CS5.1 for calculating the height of wicking front per second. Since, the multishot interval was known, i.e. one shot per second, so it was easier to calculate the wicking rate.

2.4.2. Water contact angle

The static water contact angle (WCA) was determined by Sessile drop measurements using a Contact Shape Analyzer, DSA100 (Krüss, Hamburg, Germany).

2.4.3. Diameter of nanofibers

The average diameters of nanofibers were analyzed by using Keyence Digital Microscope VH-Z500R at 5000 \times magnification.

2.4.4. Nanofibers web thickness

The average thickness of all nanofiber webs were measured by Digital Micrometer MCD130-25 with measuring sensitivity of 1 μm .

2.4.5. Scanning electron microscope

SEM (S-3000N by Hitachi, Japan) was used to study morphology of nanofiber before and after deacetylation.

2.4.6. FTIR spectroscopy

The change in chemical structure of CA nanofibers with and without blending of PVA nanofibers, before and after deacetylation, was analyzed on FTIR spectroscopy. (IR Prestige-21 by Shimadzu, Japan).

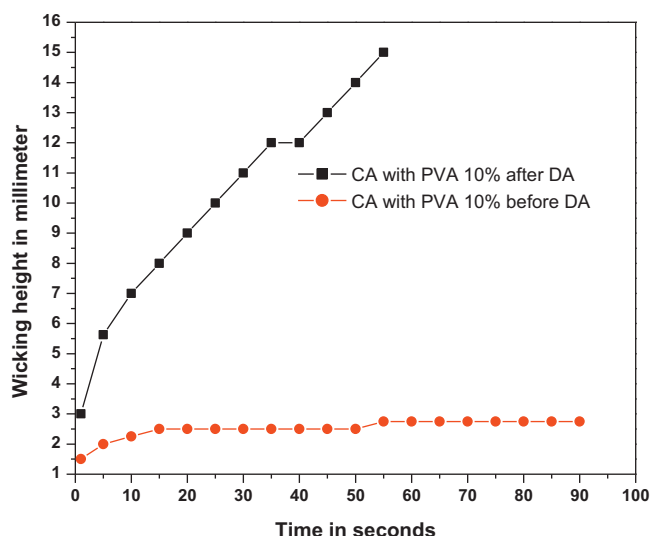


Fig. 2. Wicking rate for CA with 10% PVA, before and after deacetylation.

3. Results and discussion

3.1. Effect of deacetylation on wicking behavior of nanofiber webs

Figs. 1–3 demonstrate the wicking rate of CA and CA/PVA blend nanofibers webs, before and after deacetylation. Fig. 1 shows CA nanofibers web before and after deacetylation, almost linear with slightly decrease in wicking rate after 40 s but over all less than after deacetylation over the time. The wicking rate of deacetylated CA nanofibers web was too high initially that reached wicking front height of 7 mm within 10 s and then started decreasing slowly until 10 mm wicking front height and decreased more until the 15 mm wicking front height was reached. It can be seen that two third of wicking height was achieved in 25 s which is almost five times faster wicking rate than the remaining wicking rate and one and a half times enhanced wicking rate compared to that of the CA nanofibers web before deacetylation. The reason for the higher wicking rate is due to substitution of acetate groups with OH groups (Liu & Hsieh, 2002). This affirms the behavior of CA nanofibers after deacetylation shown in Fig. 3 at 3400 cm^{-1} .

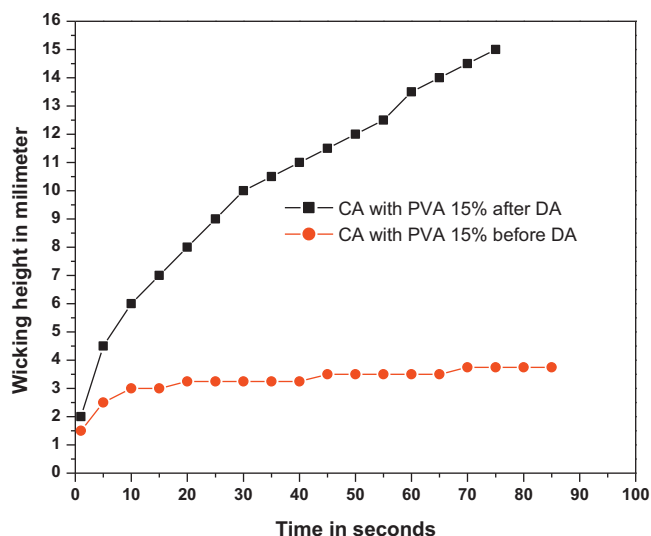








Fig. 3. Wicking rate for CA with 15% PVA, before and after deacetylation.

Figs. 2 and 3 illustrate some change in wicking behavior of CA/PVA (10%) and CA/PVA (15%) nanofiber webs before deacetylation. Wicking front height of maximum 2.5 mm and 3 mm could reach in 90 s for both PVA nanofiber samples. The reason for this decreased wicking is mainly attributed to the gel formation of PVA nanofibers that resist the liquid to flow through the web during wicking (Hodge et al., 1996). This fact is confirmed from the SEM images shown in Fig. 4(a–f), which were taken after wicking ceased. The SEM images in Fig. 4(b) and (c) clearly shows gel formation in CA/PVA (10%) and CA/PVA (15%) nanofiber webs before deacetylation. This behavior mainly attributed to the property of PVA nanofibers that have a tendency to gel formation (Hodge et al., 1996). The inset images shown in Fig. 4(a–f) are real pictures exposed during the wicking rate experiment done on all nanofiber web samples. The wicking front height of CA/PVA (15%) in Fig. 4(c) inset is relatively higher than the wicking front height of CA/PVA (10%) nanofiber web shown in Fig. 4(b). This slight enhancement is due to more PVA content in terms of nanofiber diameter resulting into many OH groups of PVA available to absorb liquid at initials wicking stage.

The PVA nanofibers were removed by deacetylation and wicking was compared before and after deacetylation. Figs. 2 and 3 depict that the wicking rate of CA/PVA (10%) and CA/PVA (15%) was significantly enhanced after deacetylation. In case of CA/PVA (10%) deacetylated nanofibers web, the wicking rate was initially too high, similar to that of the CA deacetylated nanofibers web, reaching 7 mm wicking front height within 10 s and a continuous increment up to 15 mm wicking front height within 65 s (Fig. 2). Overall, wicking was uniform and 20% faster than that of the CA deacetylated nanofibers web. In contrast to phenomenon of increased porosity in deacetylated CA nanofibers web that contributes to wicking enhancement (Callegari et al., 2011); the nanofiber web structure became denser and shrunk after the PVA component removed by deacetylation. The network of the nanofibers web was increased that provided opportunity for liquid to flow through the nanofibers web smoothly and rapidly. In addition, substitution of acetate groups of the CA with OH groups, as depicted by FTIR analysis, was also one of the main contributing factors in the enhancement of wicking front height. The CA/PVA (15%) deacetylated, on the other hand, was found to have 20% slower wicking rate than the CA/PVA (10%) deacetylated nanofibers web, in spite of more shrinkage in the nanofibers web structure. It is evident from the wicking rate data that the CA/PVA (10%) deacetylated nanofibers web had very good wicking profile.

Another method to determine the wicking behavior is water contact angle (WCA) as reported by other researchers (Liu & Chunyi, 2007; Liu & Hsieh, 2002; Liu et al., 2010). WCA was also performed for all samples and the results tabulated in Table 1. The results observed for all three types of samples were quite different from results obtained earlier using vertical capillary method for wicking. Very high average WCA of around 111.8° was obtained in case of CA nanofibers web before deacetylation. This may be attributed to the acetyl groups in CA nanofibers. This may also be due to the protruding nanofibers that resist and delay penetration of water drop into the CA nanofiber web (Sarah et al., 2011), therefore considered to be less hydrophilic. In contrast, the CA nanofiber web showed a significant increase in wicking rate provided hydrophilicity in the sample as shown in Fig. 1. The differences in obtained results are mainly due to the method principles upon which they are based. The effect of deacetylation was very significant and obvious, the WCA decreased down to 4° , nearly undetectable. The reason for this significant change was due to the acetyl group substitution with hydrophilic OH groups. The WCA of CA/PVA (10%) and CA/PVA (15%) nanofibers webs before deacetylation decreased significantly in comparison to CA nanofibers web, i.e. about nine times and ten times respectively. Table 1 depicts no significant effect of deacetylation on WCA were

Table 1
Water contact angle (°) before and after deacetylation.

Before deacetylation			After deacetylation		
CA	111.8°		CA	04°	
CA/PVA (10%)	13.6°		CA/PVA (10%)	11.3°	
CA/PVA (15%)	7.9°		CA/PVA (15%)	6.7°	

observed in both CA/PVA (10%) and CA/PVA (15%) nanofibers webs. To understand the wicking behavior of nanofibers webs, the vertical capillary method provides a better means instead of water contact angle, because the later method depends on the surface penetration only while the capillary method takes the whole nanofibers structure into account.

3.2. Effect of deacetylation on morphology of nanofibers and webs

The average diameter of nanofibers and average nanofiber web thicknesses are tabulated in Table 2. The electrospinning time for each sample was around 12 h in order to achieve 40–60 μm range of thickness. The average diameter of CA nanofibers was obtained 0.74 μm, half than the average diameter of 10% PVA nanofibers and double than the average diameter of 15% PVA nanofibers. The

diameter of PVA nanofiber is dependent upon the concentration of PVA used (Jia et al., 2007). Table 2 shows the diameter of nanofibers produced from 15% PVA was increased to almost double than the diameter of nanofibers produced from 10% PVA when the PVA concentration was increased. The effect of deacetylation on nanofiber web thickness was quite significant as shown in Table 2. Overall, the thickness of nanofibers webs was reduced after deacetylation due to shrinkage. The amount of thickness shrunk after deacetylation was around 13.6% of CA, 15.5% of CA/PVA (10%) and 16.5% of CA/PVA (15%) nanofiber webs. Slightly higher reduction in thickness after deacetylation of CA/PVA (15%) nanofiber web was due to the removal of relatively thicker diameter of 15% PVA nanofibers as compared to the diameter of 10% PVA nanofibers. In addition, sample shrinkage after deacetylation may also be the reason of overall thickness reduction.

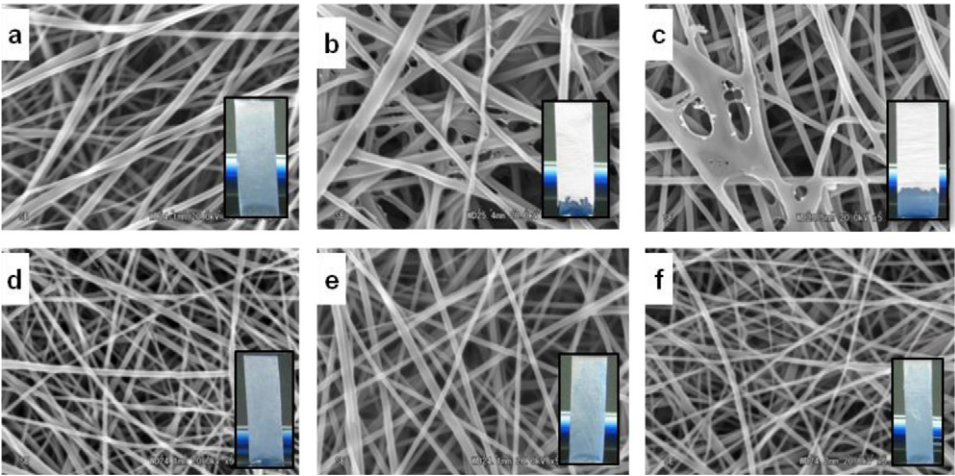


Fig. 4. SEM images taken after wicking ceased or time up. (a–c) Before deacetylation and (d–f) after deacetylation. (a) and (d) CA without PVA, (b) and (e) CA/PVA 10% and, (c) and (f) CA/PVA 15%.

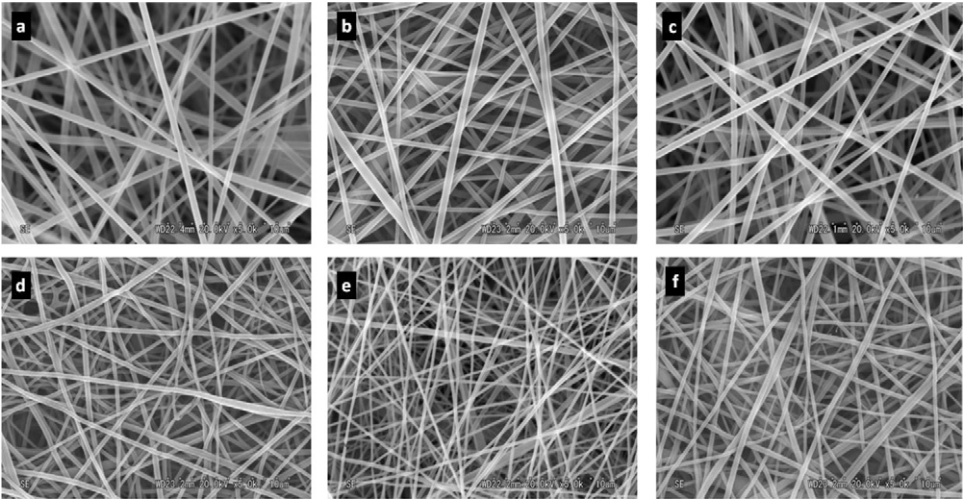


Fig. 5. SEM images (a–c) before deacetylation and (d–f) after deacetylation. (a) and (d) CA without PVA, (b) and (e) CA/PVA 10% and, (c) and (f) CA/PVA 15%.

Table 2
Nanofibers diameter and nanofibers web thickness.

Nanofibers web type	Average nanofiber diameter (μm)		Average web thickness before deacetylation (μm)	Average web thickness after deacetylation (μm)
	CA	PVA		
CA without PVA	0.74	–	44	38
CA with 10% PVA	0.74	0.34	58	49
CA with 15% PVA	0.74	0.71	60	50

The SEM images of all nanofibers webs were studied in terms of the effect of deacetylation on the nanofibers morphologies. Fig. 5(a–f) shows a significant change observed in nanofibers surface morphology after deacetylation. As reported earlier, shrinkage and increased structure density is obvious from SEM images after deacetylation.

3.3. Structural changes of deacetylated nanofibers webs

Figs. 6–8 display changes in the FTIR spectra before and after deacetylation. The intensities of characteristic adsorption peaks attributed to the vibrations of the acetate group at 1745 cm^{-1}

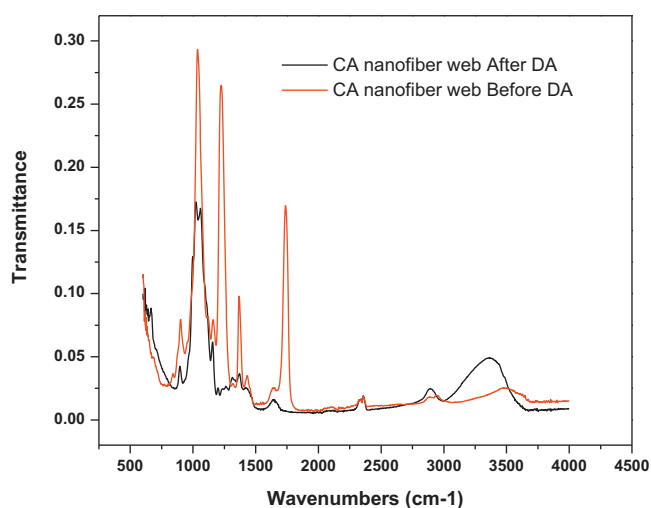


Fig. 6. FTIR for CA without PVA, before and after deacetylation.

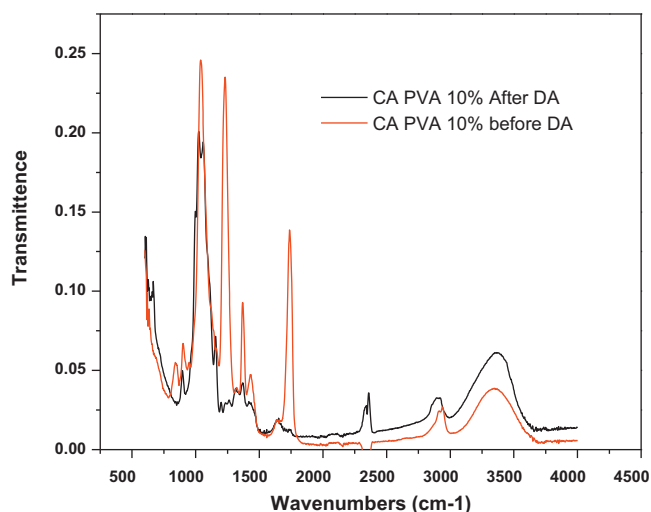


Fig. 7. FTIR for CA/PVA (10%), before and after deacetylation.

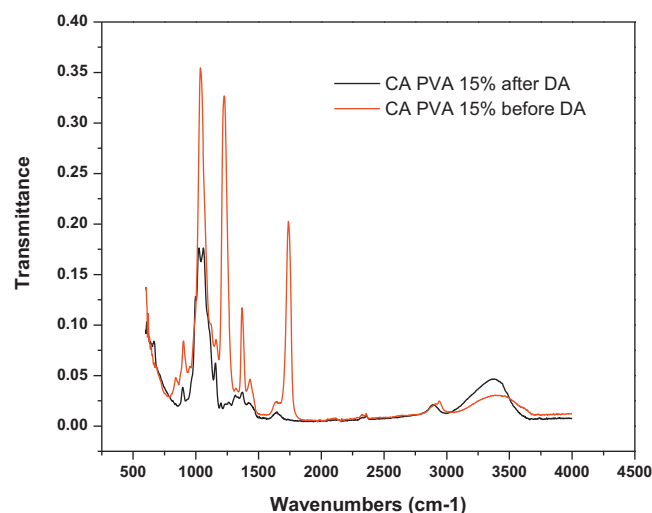


Fig. 8. FTIR for CA/PVA (15%), before and after deacetylation.

($\nu_{\text{C=O}}$), 1375 cm^{-1} ($\nu_{\text{C-CH}_3}$) and 1235 cm^{-1} ($\nu_{\text{C-O-C}}$), decreased and finally disappeared. On the contrary, an absorption peak at 3500 cm^{-1} ($\nu_{\text{O-H}}$) is increased, as shown in Figs. 7 and 8.

The PVA nanofiber has characteristic bands at around 860 cm^{-1} ($\nu_{\text{C-O}}$), 110 cm^{-1} , 1450 cm^{-1} , 2900 cm^{-1} ($\nu_{\text{C-H}_2}$) and 3400 cm^{-1} ($\nu_{\text{O-H}}$) (Ding et al., 2004). The characteristics bands at 1450 cm^{-1} , 2900 cm^{-1} ($\nu_{\text{C-H}_2}$) and 3400 cm^{-1} ($\nu_{\text{O-H}}$) became weaker and bands at 869 cm^{-1} and 110 cm^{-1} completely disappeared as result of deacetylation (Ding et al., 2004). This suggests that the PVA nanofibers after deacetylation were removed. No new peaks were observed other than common characteristic peaks of CA and PVA nanofibers, it can therefore be said that there was no chemical reaction between CA and PVA nanofibers but simply a physical blending.

4. Conclusion

The effect of deacetylation was evaluated with respect to wicking rate. Three nanofibers webs were prepared, out of which the CA/PVA (10%) nanofibers blend demonstrates faster and more uniform wicking rate as compared to the CA/PVA (15%) nanofibers blends and CA without PVA nanofibers webs. The blending of PVA nanofibers significantly decreases the wicking rate if not deacetylated. After deacetylation, all types of nanofibers webs used in this study showed overall enhanced wicking rate. The vertical capillary method provides a better understanding of wicking behavior than the water contact angle of nanofibers webs. FTIR data showed no chemical reaction between CA nanofibers and PVA nanofibers. The deacetylation had significantly affected the nanofibers web thickness, which brought a positive change in terms of increase in nanofibers network as study showed by SEM analysis. Such type of nanofibers webs can be used where the faster wicking is desired such as, biosensor strips and other medical applications.

Acknowledgement

This work was supported by Grant-in-Aid for Global COE Program by the Ministry of Education, Culture Sports Science, and Technology, Japan.

Appendix A.

CA, cellulose acetate; PVA, polyvinyl alcohol; CI, color index; WCA, water contact angle.

References

- Callegari, G., Tyomkin, I., Kornev, K. G., Neimark, A. V. & Hsieh, Y.-L. (2011). *Journal of Colloid and Interface Science*, 353, 290–293.
- Ding, B., Kimura, E., Sato, T., Fujita, S. & Shiratori, S. (2004). *Polymer*, 45, 1895–1902.
- Du, J. & Hsieh, Y.-L. (2008). *Nanotechnology*, 19, 571–579.
- Du, J. & Hsieh, Y.-L. (2009). *Cellulose*, 16, 247.
- Hodge, R. M., Edward, G. H. & Simon, G. P. (1996). *Polymer*, 37, 1371.
- Jia, Y.-T., Gong, J., Gu, X.-H., Kim, H.-Y., Dong, J. & Shen, X.-Y. (2007). *Carbohydrate Polymers*, 69, 403–409.
- Katti, D. S., Robinson, K. W., Ko, F. K. & Laurencin, C. T. (2004). *Journal of Biomedical Materials Research Part B: Applied Biomaterials*, 70B, 286.
- Liu, H. & Chunyi, T. (2007). *Polymer Journal*, 39, 65–72.
- Liu, H. & Hsieh, Y.-L. (2002). *Journal of Polymer Science Part B: Polymer Physics*, 40, 2119.
- Liu, S., Tan, L., Hu, W., Li, X. & Chen, Y. (2010). *Materials Letters*, 64, 2427–2430.
- Ma, Z. W., Kotaki, M. & Ramakrishna, S. (2005). *Journal of Membrane Science*, 265(1–2), 115–123.
- Ma, Z. W. & Ramakrishna, S. (2008). *Journal of Membrane Science*, 319, 23–28.
- Park, J. C., Ito, T., Kim, K.-O., Kim, K.-W., Kim, B.-S., Khil, M. S., et al. (2010). *Polymer Journal*, 42, 273–276.
- Sarah, J. H., Norazilawati, M.-S., Helen, J. R., Richard, L. T., Jonathan, R., William, N. A. B., et al. (2011). *Macromolecules*, 44, 6461–6470.
- Son, W. K., Youk, J. H., Lee, T. S. & Park, W. H. (2004). *Journal of Polymer Science Part B: Polymer Physics*, 42, 5–11.
- Tsukada, M., Freddi, G. & Crighiton, J. S. (1994). *Journal of Polymer Science Part B: Polymer Physics*, 32(2), 243.
- Wang, X., Kim, Y.-G., Drew, C., Ku, B.-C., Kumar, J. & Samuelson, L. A. (2004). *Nano Letters*, 4(2), 331.
- Yaser, E. G., Mohammed, A. M., Eisa, A. Al-M. & Bothaina, Al-S. (2010). *Carbohydrate Polymers*, 82, 569–577.